Theoretical Study of Stable Intermolecular Complexes of Furan with Hydrogen Halides

Dong-Mei Huang and Yi-Bo Wang*

Key Laboratory of Guizhou High Performance Computational Chemistry, Guiyang, Guizhou 55025, People's Republic of China and Department of Chemistry, Guizhou University, Guiyang, Guizhou 55025, People's Republic of China

Lisa M. Visco and Fu-Ming Tao*

Department of Chemistry and Biochemistry, California State University, Fullerton, California 92834

Received: June 1, 2004; In Final Form: August 19, 2004

The intermolecular complexes of furan with hydrogen halides are examined using ab initio calculations performed at the second-order Møller-Plesset perturbation approximation with the 6-311++G(d,p) basis set. Two types of geometry are observed: the atom-on geometry, featuring a roughly planar complex with C_{2v} symmetry and a hydrogen bond between the furan oxygen and the hydrogen halide; and the face-on geometry, in which the hydrogen halide lies above the furan ring in an orientation almost perpendicular to the plane of the ring. The furan−HF and furan−HI complexes are each found to have one minimum geometry, of the atom-on and face-on type, respectively. Both geometry types are obtained for the HCl− and HBr−furan complexes. With the exception of furan−HCl, the HX subunits of the atom-on complexes deviate slightly from the furan ring plane. Each of the face-on complexes shows interaction between the hydrogen of the halide subunit and the formal π-bond between C_2 and C_4 of the furan ring. An electrostatic density potential map of furan was generated for the determination of attractive interaction sites. Interaction energy decomposition reveals that atom-on complex interactions are predominantly electrostatic in nature, while orbital and electrostatic interactions dominate the face-on type complexes.

Introduction

The ability of π-electron systems to interact with Lewis acids has attracted attention,[1−3] because the resulting weakly bound hydrogen donor−acceptor complexes are believed to play a key role in certain chemical reactions, particularly those involving aromatic rings.[4] Heterocyclic aromatic rings and their derivatives are widely used in organic syntheses. These compounds also form weak hydrogen-bonded complexes with hydrogen halides. The importance of aromatic ring interactions, and of weakly interacting systems in general,[5] makes the understanding of the nature of such interactions indispensable.

Like all aromatic compounds, heteroaromatic rings offer a π-electron system as an attractive site for hydrogen bond formation. However, heteroaromatic rings also provide a site for hydrogen bond formation at the nonbonding electron pair (n-pair) of the heteroatom.[6−14] In the absence of the heteroatom, an above-plane structure is preferred for complex formation between aromatic compounds and hydrogen halides.[3] The presence of the n-pair binding site may pose complications in the behavior of complex formation.

Several years ago, this issue was addressed by Legon and Millen,[15] who proposed a set of rules to predict the angular geometry of complexes of the type B−HX (where X = F, Cl, Br, I, CN, CCH). These rules, which are based on the assumption that the electrophilic end of a simple acid HX seeks the region of highest electron density in the Lewis base B, state the following: (1) when the Lewis base contains only n-pairs, the Lewis acid lies along the axis of the n-pair; (2) when only π-electrons are present, the Lewis acid lies along the local symmetry axis of the π-bonding orbital; and (3) in the presence of both n-pairs and π-electrons, the angular geometry is determined by the n-pair. Subsequent studies, however, raise questions concerning the validity of these rules.[8−11]

As a typical heterocyclic aromatic compound, furan provides a useful model for the study of hydrogen-bonded complexes between heterocyclic aromatic rings and hydrogen halides (HX). Several experimental investigations into furan−HX complex formation have been undertaken recently. Shea and Kukolich[6] conducted a Fourier transform microwave spectroscopy study of furan−HCl, in which they found a hydrogen-bonded planar complex with C_{2v} symmetry and an HCl axis coincident with the internal axis of the furan ring. Lesarri et al.[7] reported similar results for furan−HF. Their molecular beam Fourier transform microwave rotational spectroscopy study found a planar hydrogen-bonded furan−HF complex with C_{2v} symmetry. In each case, hydrogen bond formation occurred at the site of the furan O atom. Analysis of the rotational spectrum of furan−HBr by Legon et al.[8] revealed a weakly hydrogen-bonded complex with a face-on geometry, in which the HBr subunit lies almost perpendicular to the ring plane. With complex formation directed by the π-electrons rather than the n-pair, the behavior of furan−HBr appears to be an exception to the aforementioned rules in the prediction of B−HX geometries. Legon et al.[8] explained that the smaller dipole moment of HBr (than that of HCl or HF) was responsible for the observed structure of furan−HBr.

The discrepancies between the experimental results and the rules proposed to predict the angular geometry of B−HX complexes demonstrate the need for further study of hydrogen-

* Corresponding authors. Email: ybw@gzu.edu.cn (Y.B.W.) and ftao@fullerton.edu (F.M.T.).

10.1021/jp047636n CCC: $27.50
Published on Web 11/24/2004

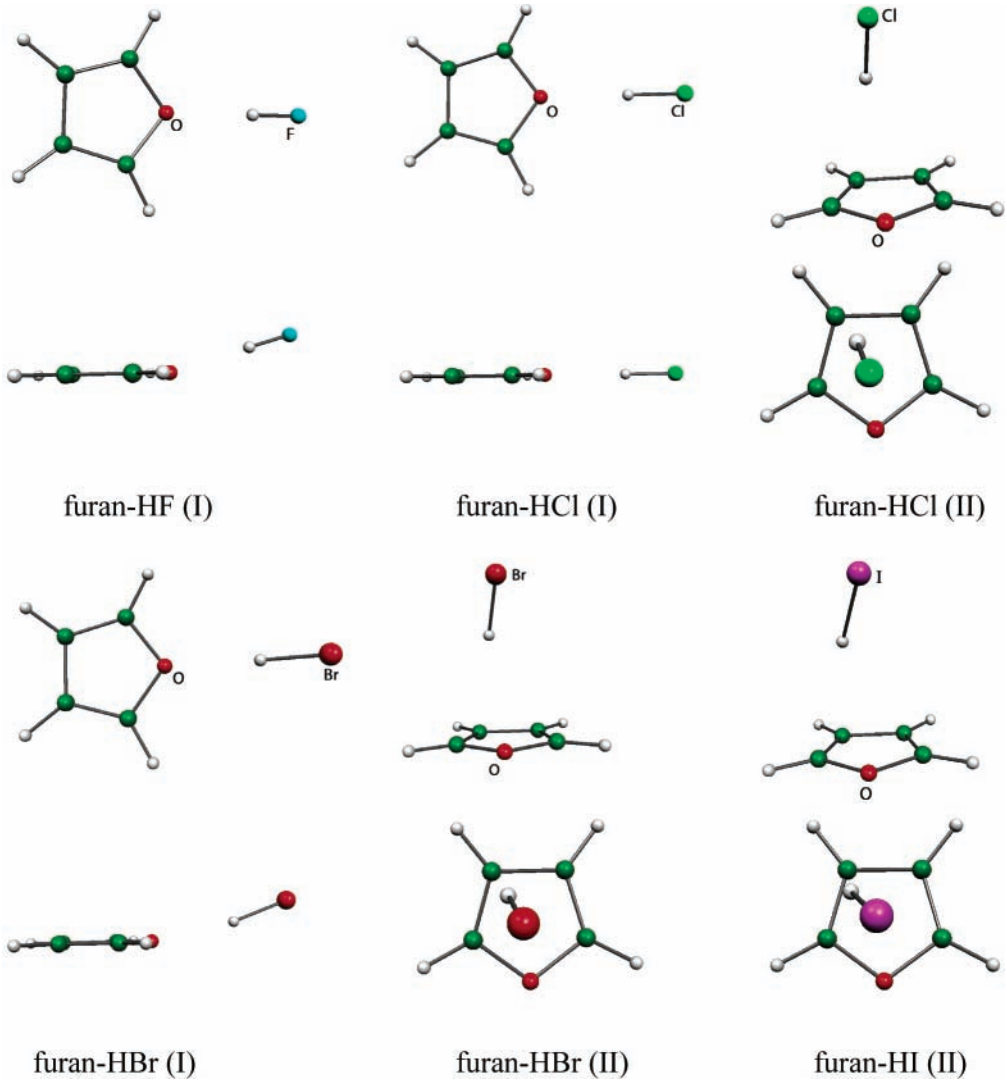

Figure 1. Minimum-energy geometries obtained for furan−HX complexes using the MP2 theoretical method with the 6-311++G(d,p) basis set (side and top views are shown).

bonded heteroaromatic ring complexes. In addition, interaction energy data, which may potentially enhance the understanding of the behavior of such ring complexes, is still not available at present. Furthermore, no study has been reported on the complex of furan with HI, the next hydrogen halide after HBr along the series. The present study is intended to resolve the ambiguities surrounding the structure and stability of the furan−HX complexes. Equilibrium geometries, intermolecular energies and their components, and harmonic frequencies are presented for all stable complexes of furan with the four hydrogen halides, HF, HCl, HBr, and HI.

Computational Methods

Equilibrium geometries of the monomers and complexes were fully optimized with the 6-311++G(d,p) basis set[17] at the second-order Møller-Plesset (MP2) level[18] using the *Gaussian 98* program package.[16] Harmonic frequencies were calculated to confirm the equilibrium geometries that correspond to energy minima. The intermolecular energies between furan and HX at the equilibrium geometries were calculated at the MP2/6-311++G(3d,3p) level. The full counterpoise method[19] was used to consider the effect of the basis set superposition error (BSSE) on the calculated intermolecular energies. The extended transition state method[20] in ADF2002.2[21] was employed for the interaction energy decomposition, performed using a valence triple-ζ polarized Slater-type orbital (STO) basis set and the Perder-Wang density functional (PW91) theory.[22] The molecular electrostatics potential map (MEP) of furan was calculated at the MP2/6-311++G(d,p) level and plotted using *Molekel 4.2*.[23]

Results and Discussion

The equilibrium geometries of the furan−HX complexes are shown in Figure 1. These geometries are classified as either atom-on or face-on types (also referred to in this paper as geometry types I and II, respectively). The atom-on type geometry is characterized by a hydrogen bond formed at the furan oxygen, with HX lying along the C_{2v} axis of furan. This geometry type is observed for the furan−HF, −HCl, and −HBr complexes (Figure 1). Furan−HCl and furan−HBr also have equilibrium geometries of the face-on type. The face-on geometry features a hydrogen bond between the hydrogen halide and the π-electron system of the aromatic ring. In this geometry, the halide lies almost directly above the center of the ring, while the hydrogen atom is oriented toward the edge of the furan ring. Structural parameters of these two types are summarized in Tables 1 and 2 and compared with available experimental data. Definitions of the geometrical parameters and atomic labeling schemes for the atom-on and face-on type complexes are presented in Figures 2 and 3, respectively.

TABLE 1: Geometric Parameters for Atom-On Type (Type I) Furan−HX Complexes Optimized at the MP2/6-311++G(d,p) Level[a]

	furan−HF	furan−HCl	furan−HBr
R_{H-O}	1.8018	1.9868	2.0445
R_{H-O}*	1.7873[b]		
	1.7940[b]		
R_{X-O}	2.7282	3.2618	3.4559
R_{X-O}*		3.26(1)[c]	
$R_{C.M.}$	3.7628	4.3498	4.5464
$R_{C.M.}$*	3.8000[b]	4.3588[c]	
	3.8067[b]	4.3686[c]	
$\theta_{(X-H-O)}$	179.0	172.5	171.7
$\theta_{(H-O-B)}$	11.6	0.7	8.6
$\theta_{(B-O-D)}$	1.2	0.0	1.4

[a] Distances (Å) and angles (°) are shown, along with available experimental data (indicated by asterisk). [b] Reference 7. [c] Reference 6.

TABLE 2: Geometric Parameters for Face-On Type (Type II) Furan−HX Complexes Optimized at the MP2/6-311++G(d,p) Level[a]

	furan−HCl	furan−HBr	furan−HI
R_{H-O}	2.7856	2.7824	2.7603
R_{H-O}*		2.599(3)[b]	
R_{H-C2}	2.4652	2.4949	2.5500
R_{H-C3}	2.6140	2.6703	2.7918
R_{H-C4}	2.5738	2.5656	2.5278
R_{H-C5}	2.7890	2.8223	2.8918
R_{H-B}	2.4249	2.4357	2.4445
$R_{C.M.}$	3.4499	3.6507	3.8201
θ_{X-A-B}	89.4	90.2	92.4
θ_{H-B-A}	75.6	76.4	78.5
θ_{X-H-B}	156.4	159.3	161.1
$\phi_{H-C-A-B}$	46.4	39.0	23.5

[a] Distances (Å) and angles (°) are shown, along with available experimental data (indicated by asterisk). [b] Reference 8.

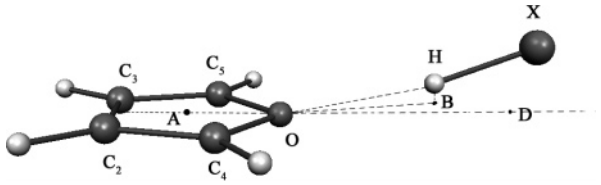

Figure 2. Definition of the geometric parameters of the atom-on (or type I) furan−HX complexes. The angle θ_{H-O-D} defines the in-plane deviation from the C_{2v} axis of furan; the out-of-plane deviation from the C_{2v} axis direction is defined by θ_{H-O-B}.

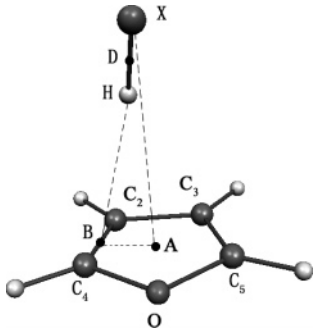

Figure 3. Definition of points A, B, and C and the atom serial numbers of the face-on (or type II) furan−HX complex geometry.

Table 1 shows the hydrogen bond lengths R_{H-O}'s, oxygen−halide distances R_{X-O}'s, and center-of-mass distances $R_{C.M.}$'s for the atom-on type complexes. For furan−HF (I), the calculated R_{H-O} and $R_{C.M.}$ values, 1.8018 and 3.7628 Å respectively, compare favorably with the available experimental data.[7] For furan−HCl (I), the calculated R_{X-O} and $R_{C.M.}$ values, 3.2618 and 4.3588 Å respectively, are also in good agreement with the experimental data.[6] As expected, all bond distances are shown to increase with the atomic number of the halide. The bond angle $\theta_{(X-H-O)}$, the in-plane deviation of HX from the C_{2v} axis of furan $\theta_{(B-O-D)}$, and the out-of-plane deviation of HX from the furan plane $\theta_{(H-O-B)}$ are also tabulated. The atom-on complex parameters in Table 1 indicate that nearly linear hydrogen bonds are formed between the furan and the HX subunits with $\theta_{(X-H-O)}$ values greater than 171°. The $\theta_{(H-O-B)}$ and $\theta_{(B-O-D)}$ angles show the HX subunits lying along the C_{2v} axis of furan and deviating slightly from the furan ring plane, a result which differs somewhat from experimental observations.[6,7]

All of the face-on type complexes exhibit C_1 symmetry. Geometric parameters are employed to define the two subunits and their relative orientation in space. The distances between the H atom of the hydrogen halide and the carbon atoms of the furan ring are listed in Table 2. The distance between the center of mass of furan and that of HX is defined by $R_{C.M.}$. The R_{H-B} value denotes the distance between the H atom of the hydrogen halide and the midpoint of C_2-C_4 bond, represented by point B (Figure 3). Points A and C are the geometric centers of the furan and HX molecules, respectively. For each of the face-on type complexes, R_{H-B} is the shortest distance between the hydrogen of the hydrogen halide and the furan ring (Table 2). This is consistent with the observation that the HX subunit is directed toward the C_2-C_4 bond of the furan ring. The relative orientation of the subunits is therefore described by the angles $\theta_{(X-A-B)}$, $\theta_{(H-B-A)}$, and $\theta_{(X-H-B)}$ and the dihedral angle $\phi_{(H-C-A-B)}$. The angle $\theta_{(X-A-B)}$ is approximately 90° for each complex, indicating that the halide atom lies almost directly above the center of the furan ring. The angle $\theta_{(H-B-A)}$ is less than 80° for each complex. We note from the dihedral angle $\phi_{(H-C-A-B)}$ that the H atom leans slightly toward the C_2 atom for all complexes. It is clear that the HX subunit interacts with the π-electron density near the C_2-C_4 bond. This contradicts the rules proposed by Legon et al., which would predict hydrogen bond formation at the furan oxygen.[15] While in general agreement with experimental results, the geometry of furan−HBr (II) differs with respect to the distance between the furan oxygen and the hydrogen atom of the HX subunit. The calculated R_{H-O} distance of 2.7824 Å is greater than the experimental value (2.5993 Å).[8] It should be noted that two possible values for the angle of the HX unit with respect to the furan axis, $\alpha_{az} = 11.9°$ and $-11.9°$, are consistent with the experimental observations. Additionally, one could also expect large-amplitude zero-point vibrations involving the HX unit. After consideration of all these effects on the observed geometry, the calculated R_{H-O} distance is in reasonable agreement with the experimental result.

Interaction energies ΔE, basis set superposition error (BSSE) values, counterpoise corrected interaction energies ΔE^{CP}, zero point energies (ZPE), and energies corrected for both the ZPE and BSSE were calculated at the MP2/6-311++G(d,p) level for each of the furan−HX complexes (Table 3). Interaction potentials, BSSE values, and counterpoise corrected interaction potentials, calculated at the MP2/6-311++G(2d,3p) and MP2/aug-cc-pVTZ levels, are also presented in Table 3. All of the interaction potentials, both corrected and uncorrected, show that the strongest bond is formed between furan and HF; with the exception of ΔE^{CP+ZPE}, each of these interaction potentials is at least −4.88 kcal/mol, indicating a strong hydrogen bond for this atom-on type complex. Among the three atom-on type

TABLE 3: Interaction Energies ΔE, BSSE, Interaction Energies Corrected for BSSE ΔE^{CP}, ZPE, and Interaction Energies Corrected for Both BSSE and ZPE ΔE^{CP+ZPE}[a]

	furan−HF (I)	furan−HCl (I)	furan−HCl (II)	furan−HBr (I)	furan−HBr (II)	furan−HI (II)
			MP2/6-311++G**			
ΔE	−6.66	−4.91	−5.01	−4.24	−4.85	−4.84
BSSE	1.78	1.90	2.54	1.62	2.92	2.39
ΔE^{CP}	−4.88	−3.01	−2.47	−2.62	−2.56	−2.45
ZPE	2.42	1.11	1.18	1.08	1.12	1.13
ΔE^{CP+ZPE}	−2.46	−1.90	−1.29	−1.54	−1.43	−1.32
			MP2/6-311++G(3d,3p)			
ΔE	−6.71	−4.62	−5.51	−3.95	−5.28	−5.73
BSSE	1.48	1.13	1.77	0.92	1.56	2.33
ΔE^{CP}	−5.23	−3.49	−3.74	−3.03	−3.72	−3.40
			MP2/aug-cc-pvTZ			
ΔE	−6.36	−4.54	−5.04	−4.71	−5.87	
BSSE	0.79	0.69	0.87	1.27	1.62	
ΔE^{CP}	−5.57	−3.85	−4.17	−3.43	−4.25	

[a] All energies are in kcal/mol.

complexes, the interaction potential is shown to decrease as atomic number/radius increases.

In contrast to the atom-on type complexes, the face-on complexes show interaction potentials that are almost isoenergetic (Table 3). At the MP2/6-311++G(d,p) level, the identity of the halide atom has little effect on the interaction potentials, ΔE, ΔE^{CP}, and ΔE^{CP+ZPE}. For 6-311++G(3d,3p) and the correlation-consistent basis set, greater variation is observed among the ΔE values for furan−HCl, −HBr, and −HI. However, these differences narrow when the interaction potentials are corrected for the BSSE.

For clusters with both atom-on and face-on type geometry minima, the strongest interaction potentials are generally observed for the face-on type complexes. This is true of all interaction potentials calculated at the MP2/6-311++(3d,3p) and MP2/aug-cc-pVTZ levels. However, calculations performed at the MP2/6-311++G(d,p) level give mixed results with the atom-on complexes showing stronger ΔE^{CP} and ΔE^{CP+ZPE} values than the face-on types. From the detailed analysis, it seems reasonable to conclude from Table 3 that the geometry is transformed from the atom-on type to face-on type for furan−HX complexes in the sequence X = F, Cl, Br, and I.

Like benzene, furan is an aromatic compound with a delocalized π-electron system. However, the aromaticity of furan is weaker than that of benzene because of the relatively strong electronegativity of its O atom and the bond angle $\theta_{(C-O-C)}$, which, at 107°, is larger than the ideal angle of 60°. As a result, a large electron density is conferred on the O atom. Evidence of this is provided by the MEP map of furan, shown in Figure 4. The MEP plot indicates a positive electrostatic potential (shown in blue), corresponding to the regions of the furan hydrogen atoms. Around the O atom and along the C_2-C_3 bonds, regions of negative electrostatic potential (shown in red) are noticeable, with the strongest negative potential in the immediate vicinity of the O atom. This result, while in accordance with the atom-on type complexes, seems to imply that, for the face-on type complexes, the H atom of HX should point in the direction of the strong negative potential on the O atom. Instead, the H atom is shown to favor the π-electron density of the C−C bond, suggesting that the primary intermolecular attraction for the face-on complexes is not electrostatic in nature.

Therefore, the nature of the interaction was further investigated by interaction energy decomposition. By using the extended transition state method in ADF2002.2, the interaction

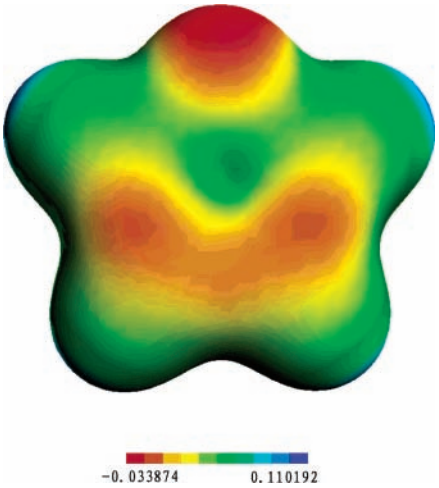

Figure 4. Molecular eletrostatic potential map of furan from −0.033 874 to +0.110 192 e/$4\pi\varepsilon_0 a_0$, onto 0.008 e Å^{-3} m, isosurface of the electron density at the MP2/6-311++G(d,p) level.

TABLE 4: Energy Decompositions Calculated at PW91/TZP Level[a]

	furan−HF (I)	furan−HCl (I)	furan−HCl (II)	furan−HBr (I)	furan−HBr (II)	furan−HI (II)
ΔE_{Pauli}	7.52	5.70	4.01	5.10	4.13	4.73
$\Delta E_{elestat}$	−7.76	−5.33	−3.38	−4.59	−3.24	−3.38
ΔE_{orbi}	−6.22	−3.89	−3.41	−3.58	−3.56	−3.46
ΔE_{Int}	−6.46	−3.52	−2.78	−3.08	−2.67	−2.11
ΔE_{orbi}%[b]	44	42	50	44	52	51

[a] Energies are in kcal/mol. [b] ΔE_{orbi}% is the percentage of the total interaction energy contributed by the orbital component.

energy ΔE was decomposed into electrostatic interaction $\Delta E_{elestat}$, orbital ΔE_{orbi}, and Pauli-repulsion ΔE_{Pauli} terms. All calculations were performed for the optimized geometries using ADF2002.2 at the PW91/TZP level. The energy decompositions and the total interaction energies are listed in Table 4, together with the percentage of the total attractive interaction energy, contributed by the orbital component. The results in Table 4 show that, for all complexes, both the electrostatic and orbital interaction terms are attractive, while the Pauli term, which accounts for the interaction between closed shells, is repulsive. In the case of the atom-on type complexes, the electrostatic term contributes 57−60% of the total attractive interaction. Each of the interaction components decreases significantly when going from furan−HF (I) to furan−HBr (I). The total interaction energy follows the same trend. But, in the case of three face-on type complexes, electrostatic interaction and orbital interaction each contribute approximately 50% to the total attraction. The Pauli repulsive interaction increases slightly with the atomic number of the halide. The relative changes in the three components of the interaction energy indicate that the interaction energy decreases slightly from furan−HCl (II) to furan−HI (II). It is clear from the energy decomposition data that the nature of the interaction is different for the two complex types. For atom-on type complexes, the electrostatic component predominates in complex formation. Face-on type complexation is governed by orbital and electrostatic interactions.

As expected, furan−HX complexation of both types produces significant changes in the HX subunit. The H−X bond length increases upon complex formation. The most dramatic increase (from 0.9166 to 0.9265 Å) occurs when fluorine is the halide atom (Table 5). Bond length increases of more than 0.0060Å are observed for the remaining HX subunits. This validates the common-sense intuition that the HX moiety plays the most

TABLE 5: Bond Lengths (Å) and Harmonic Stretching Vibrational Frequencies (cm^{-1}) of Free and Bound HX Subunits Calculated at the MP2/6-311++G(d,p) Level[a]

	furan−HF (I)	furan−HCl (I)	furan−HCl (II)	furan−HBr (I)	furan−HBr (II)	furan−HI (II)
R_{comp}	0.9265	1.2816	1.2798	1.4201	1.4195	1.6127
R_{free}	0.9166	1.2732	1.2732	1.4124	1.4124	1.6054
ΔR	0.0099	0.0084	0.0066	0.0077	0.0071	0.0073
υ_{comp}	3286	2974	2998	2651	2658	2342
υ_{free}	4198	3087	3087	2738	2738	2371
$\Delta\upsilon$	911	112	88	87	80	29

[a] The differences between the free and bound bond lengths and frequencies are also shown.

important role in the formation of the hydrogen bond, a point confirmed by our vibrational frequency calculations. From the calculated harmonic frequencies of the H−X stretching mode in the complexes and free monomers, red-shifts have been obtained for each of the complexes (Table 5). In accordance with the interaction energies, the extent of the red-shift is shown to decrease in sequence from HF to HI, regardless of the geometry type.

Conclusion

The weakly hydrogen-bonded complexes formed by furan and the hydrogen halides have two geometry types. One is the atom-on type, in which the H atom of HX interacts with the nonbonding electron pairs of the furan O atom. In this complex type, the HX subunit lies along the C_{2v} axis of the furan, deviating slightly from the furan ring plane. The other geometry is the face-on type, which features a hydrogen bond between the H atom of HX and the π-electron system of the aromatic heterocycle. The geometries transformed from the atom-on type to the face-on type progressively along the series of HF, HCl, HBr, and HI. The atom-on type complexes are traditional hydrogen-bonded complexes with electrostatic interactions making the primary contribution to complex formation. In the case of the face-on type complexes, orbital and electrostatic forces dominate complexation, resulting in the H atom of the HX subunit favoring the unsaturated C−C bond near the β-C atom of furan, rather than the furan O atom.

The present theoretical results are in overall good agreement with available experimental observations. There are still some discrepancies with the details from experiment. It is hoped that the insights provided herein will assist experimental workers in their efforts to resolve the remaining matter of hydrogen-bonded complexes involving molecules that exhibit both π-electron systems and nonbonding electron pairs.

Acknowledgment. This work was supported by The National Natural Science Foundation of China (No. 20463002), The Stadholder Foundation of Guizhou Province, and The Camille and Henry Dreyfus Foundation (Award No. TH-00-028).

References and Notes

(1) (a) Kim, K. S.; Tarakeshwar, P. J.; Lee, Y. *Chem. Rev.* **2000**, *100*, 4145. (b) Brutschy, B. *Chem. Rev.* **2000**, *100*, 3891.

(2) (a) Casassa, M. P.; Western, C. M.; Celii, F. G.; Brinza, D. E.; Janda, K. C. *J. Chem. Phys.* **1983**, *79*, 3227. (b) Tachikawa, H. *Phys. Chem. Chem. Phys.* **2000**, *2*, 839. (c) Carcabal, P.; Broquier, M.; Picard-Bersellini, A.; Brenner, V.; Millie, P. *J. Chem. Phys.* **2000**, *113*, 4876. (d) Carcabal, P.; Seurre, N.; Chevalier, M.; Broquier, M.; Brenner, V. *J. Chem. Phys.* **2002**, *117*, 1522. (e) Mootz, D.; Deeg, A. *J. Am. Chem. Soc.* **1992**, *114*, 5887. (f) McDowell, S. A. C. *Phys. Chem. Chem. Phys.* **2001**, *3*, 2754. (g) Prieto, P.; De la Hoz, A.; Alkorta, I.; Rozas, I.; Elguero, J. *Chem. Phys. Lett.* **2001**, *350*, 325. (h) Read, W. G.; Flygare, W. H. *J. Chem. Phys.* **1982**, *76*, 2238. (i) Legon, A. C.; Aldrich, P. D.; Flygare, W. H. *J. Chem. Phys.* **1981**, *75*, 625. (j) Kolenbrander, K. D.; Lisy, J. M. *J. Chem. Phys.* **1986**, *85*, 2463. (k) Huang, Z. S.; Miller, R. E. *J. Chem. Phy.* **1987**, *86*, 6059. (l) Andrews, L.; Johnson, G. L.; Kelsall, B. J. *J. Phys. Chem.* **1991**, *95*, 2881. (m) Dayton, D. C.; Block, P. A.; Miller, R. E. *J. Phys. Chem.* **1982**, *86*, 3374. (n) Oudejans, L.; Miller, R. E. *J. Phys. Chem. A* **1999**, *103*, 4791. (o) Hinchliffe, A. *Chem. Phys. Lett.* **1982**, *85*, 531. (p) Pople, J. A.; Frisch, M. J.; Del Bene, J. E. *Chem. Phys. Lett.* **1982**, *91*, 185. (q) De Almeida, W. B.; Hinchliffe, A. *Chem. Phys.* **1989**, *137*, 143. (r) Bacskay, G. B.; Kerdraon, D. I.; Hush, N. S. *Chem. Phys.* **1990**, *144*, 53. (s) Araujo, R. C. M. U.; Da Silva, J. B. P.; Ramos, M. N. *Spectrochim. Acta, Part A* **1995**, *51*, 821. (t) Jeomg, H. Y.; Han, Y.-K. *Chem. Phys. Lett.* **1996**, *263*, 345. (u) Abrash, S. A.; Carr, C. M.; McMahon, M. T.; Zehner, R. W. *J. Phys. Chem.* **1994**, *98*, 11909. (v) Tantriungrotechai, Y.; Tonmunphean, S.; Wihitkosoom, A. *Phys. Chem. Chem. Phys.* **2002**, *4*, 4619. (w) Read, W. G.; Campbell, E. J.; Henderson, G.; Flygare, W. H. *J. Am. Chem. Soc.* **1981**, *103*, 7670. (x) Resd, W. G.; Campbell, E. J.; Henderson, G. *J. Chem. Phys.* **1983**, *78*, 3501. (y) Bredas, J. L.; Street, G. B. *J. Am. Chem. Soc.* **1988**, *110*, 7001.

(3) (a) Rozas, I.; Alkorta, I.; Elguero, J. *J. Phys. Chem. A* **1997**, *101*, 9457. (b) Tarakeshwar, P.; Lee, S. J.; Kim, K. S. *J. Chem. Phys.* **1998**, *108*, 7217. (c) Deeg, A.; Mootz, D. *Z. Naturforsch., B: Chem. Sci.* **1993**, *48*, 571. (d) Cooke, S. A.; Corlett, G. K.; Evans, C. M.; Legon, A. C. *Chem. Phys. Lett.* **1997**, *272*, 61. (e) Read, W. G.; Campbell, E. J.; Henderson, G.; Flygare, W. H. *J. Am. Chem. Soc.* **1981**, *103*, 7670. (f) See, for example, Mulliken, R. S.; Person, W. B. Molecular Complexes; Wiley-Interscience: New York, 1969; and references therein. (g) Hassel, O.; Strømme, K. *Acta Chem. Scand.* **1985**, *12*, 1146. (h) Fredin, L.; Nelander, B. *J. Am. Chem. Soc.* **1974**, *96*, 1672. (i) Fredin, L.; Nelander, B. *Mol. Phys.* **1974**, *77*, 885. (j) Bai, H.; Ault, B. S. *J. Phys. Chem.* **1990**, *94*, 199. (k) See, for example, Hassel, O.; Rømming, C. *Q. Rev. Chem. Soc.* **1962**, *14*, 1. (l) Walters, E. A.; Grover, J. R.; White, M. G.; Hui, E. T. *J. Phys. Chem.* **1985**, *89*, 3814. (m) Gord, J. R.; Garrett, A. W.; Bandy, R. E.; Zwier, T. S. *Chem. Phys. Lett.* **1990**, *171*, 443. (n) Gotch, A. S.; Zwier, T. S. *J. Chem. Phys.* **1990**, *93*, 6977. (o) Baiocchi, F. A.; Williams, J. H.; Klemperer, W. *J. Phys. Chem.* **1983**, *87*, 2079. (p) Sapse, A. M.; Jain, D. C. *J. Phys. Chem.* **1984**, *88*, 4970. (q) Cheney, B. V.; Schulz, M. W. *J. Phys. Chem.* **1990**, *94*, 6268.

(4) (a) Mulliken, R. S. *J. Am. Chem. Soc.* **1950**, *72*, 600. (b) Foster, R. S. *Organic Charge Transfer Complexes*; Academic Press: New York, 1969. (c) Loudon, G. M. *Organic Chemistry*, 2nd ed.; Benjamin Cummings: Menlo Park, NJ, 1988.

(5) Desiraju, G. R.; Steiner, T. *The weak bond hydrogen bond in structural chemistry and biology*; Oxford University Press: Oxford, 1990.

(6) Shea, J. A.; Kukolich, S. G. *J. Chem. Phys.* **1983**, *78*, 3545.

(7) Lesarri, A.; López, J. C.; Alonso, J. L. *J. Chem. Soc., Faraday Trans.* **1998**, *94*, 729.

(8) Cole, G. C.; Legon, A. C.; Ottaviani, P. *J. Chem. Phys.* **2002**, *117*, 2790.

(9) Cooke, S. A.; Corlett, G. K.; Legon, A. C. *Chem. Phys. Lett.* **1998**, *291*, 269.

(10) Cooke, S. A.; Corlett, G. K.; Legon, A. C. *J. Chem. Soc., Faraday Trans.* **1998**, *94*, 1565.

(11) Cooke, S. A.; Holloway, J. H.; Legon, A. C. *Chem. Phys. Lett.* **1998**, *298*, 151.

(12) Jiang, J. C.; Tsai, M.-H. *J. Phys. Chem. A* **1997**, *101*, 1982.

(13) Cooke, S. A.; Corlett, G. K.; Legon, A. C. *J. Mol. Struct.* **1998**, *448*, 107.

(14) Cooke, S. A.; Corlett, G. K.; Lister, D. G.; Legon, A. C. *J. Chem. Soc., Faraday Trans.* **1998**, *94*, 837.

(15) (a) Legon, A. C.; Millen, D. J. *Faraday Discuss. Chem. Soc.* **1982**, *73*, 71. (b) Legon, A. C.; Millen, D. J. *Chem. Soc. Rev.* **1987**, *16*, 467.

(16) Frisch, M. J.; Trucks, G. W.; Schlegel, H. B.; Scuseria, G. E.; Robb, M. A.; Cheeseman, J. R.; Zakrzewski, V. G.; Montgomery, J. A., Jr.; Stratmann, R. E.; Burant, J. C.; Dapprich, S.; Millam, J. M.; Daniels, A. D.; Kudin, K. N.; Strain, M. C.; Farkas, O.; Tomasi, J.; Barone, V.; Cossi, M.; Cammi, R.; Mennucci, B.; Pomelli, C.; Adamo, C.; Clifford, S.; Ochterski, J.; Petersson, G. A.; Ayala, P. Y.; Cui, Q.; Morokuma, K.; Malick, D. K.; Rabuck, A. D.; Raghavachari, K.; Foresman, J. B.; Cioslowski, J.; Ortiz, J. V.; Stefanov, B. B.; Liu, G.; Liashenko, A.; Piskorz, P.; Komaromi, I.; Gomperts, R.; Martin, R. L.; Fox, D. J.; Keith, T.; Al-Laham, M. A.; Peng, C. Y.; Nanayakkara, A.; Gonzalez, C.; Challacombe, M.; Gill, P. M. W.; Johnson, B. G.; Chen, W.; Wong, M. W.; Andres, J. L.; Head-Gordon, M.; Replogle, E. S.; Pople, J. A. *Gaussian 98*; Gaussian, Inc.: Pittsburgh, PA, 1998.

(17) Krishnam, R.; Binkley, J. S.; Seeger, R.; Pople, J. A. *J. Chem. Phys.* **1984**, *80*, 3265.

(18) Møller, C.; Plesset, M. S. *Phys. Rev.* **1934**, *46*, 618.

(19) Boys, S. B.; Bernardi, F. *Mol. Phys.* **1970**, *19*, 553.

(20) (a) Ziegler, T.; Rauk, A. *Inorg. Chem.* **1979**, *18*, 1558. (b) Ziegler, T.; Rauk, A. *Inorg. Chem.* **1979**, *18*, 1755. (c) Bickelhaup, F. M.; Baerends, E. J. *Rev. Comput. Chem.* **2000**, *15*, 1. (d) Fonseca Guerra, C.; Bickelhaupt, F. M. *Angew. Chem. Int. Ed.* **2002**, *41*, 2092. (e) Wang, Y.-B.; Lin Z. *J. Am. Chem. Soc.* **2003**, *125*, 6072.

(21) (a) te Velde, G.; Bickelhaupt, F. M.; van Gisbergen, S. J. A.; Fonseca Guerra, C.; Baerends, E. J.; Snijders, J. G.; Ziegler, T. *J. Comput. Chem.* **2001**, *22*, 931. (b) Fonseca Guerra, C.; Snijders, J. G.; te Velde, G.; Baerends, E. J. *Theor. Chem. Acc.* **1998**, *99*, 391.

(22) Perdew, J. P.; Chevary, J. A.; Vosko, S. H.; Jackson, K. A.; Pederson, M. R.; Singh, D. J.; Fiolhais, C. *Phys. Rev. B* **1992**, *46*, 6671.

(23) Flükiger, P.; Lüthi, H. P.; Portmann, S.; Weber, J. *MOLEKEL* version 4.2; Swiss Center for Scientific Computing: Manno, 2000.